Ceramics International xxx (xxxx) xxx–xxx

Contents lists available at ScienceDirect

Ceramics International

journal homepage: www.elsevier.com/locate/ceramint

Short communication

Influence of substrate and sintering temperature on the thickness and number of layers of 3YSZ multilayer sol-gel coatings

Juan P. Carrasco-Amador[a], María A. Díaz-Díez[b], José Sánchez-González[b], Antonio Díaz-Parralejo[b], Angel L. Ortiz[b,*]

[a] Departamento de Expresión Gráfica, Universidad de Extremadura, 06006, Badajoz, Spain
[b] Departamento de Ingeniería Mecánica, Energética y de los Materiales, Universidad de Extremadura, 06006, Badajoz, Spain

ARTICLE INFO

Keywords:
Sol-gel
Dip-coating
Zirconia
Thin films/coatings
Sintering temperature

ABSTRACT

A study was made of the influence of the substrate (fused quartz, sapphire, soda-lime glass, and stainless steel AISI-310) and sintering temperature (300 °C, 500 °C, and 800 °C) on the thickness and number of layers of 3YSZ multilayer sol-gel coatings that can be deposited by dip-coating without the coating cracking. It was found that the thickness and the number of layers increase with the higher sintering temperature and the greater substrate's thermal expansion coefficient. These trends were explained as resulting from the residual in-plane stresses generated in the sol-gel coating when cooled from the sintering temperature down to room temperature due to its thermal expansion coefficient differing from that of the substrate. Thus, the smaller the residual in-plane tensile stress or the greater the residual in-plane compressive stress, the greater can be the thickness and number of layers of the sol-gel coating. The same is the case for higher sintering temperatures because the densification of the layers either predominates over the increased in-plane tensile stresses or combines synergistically with the greater in-plane compressive stresses.

1. Introduction

Due to their excellent combination of physicochemical properties (such as high hardness and stiffness, great refractoriness, low thermal conductivity, high chemical inertness, etc.), ceramic coatings are widely used as thermal protection, anti-wear/impact, and anti-corrosion/oxidation barriers. Ceramic coatings based on Y_2O_3-stabilized ZrO_2 (YSZ) are in particular demand not only because they offer all these protections simultaneously (as a consequence of their low thermal conductivity, high melting point, hardness and toughness, and oxidic nature) [1,2] but also for their optical properties. For example, YSZ is the commonly used composition for the current thermal barrier coatings. The YSZ films are also used for solid oxide fuel cells, in catalysis applications, for dental restorations and prostheses, etc.

The sol-gel method is ideal for preparing thin coatings of oxidic ceramics, with its suitability and versatility having been clearly demonstrated [3]. Its advantages include low processing temperatures, precise control of the chemical composition, excellent adhesion to the substrate, etc. [4]. Dip-coating stands out among the possible ways to deposit sol-gel ceramic coatings because it allows large surfaces to be covered, uses very simple equipment, and is of low cost [5,6], to name just a few of its advantages.

The quality of sol-gel coatings is key to their functionality and durability. For example, cracks degrade their mechanical properties and consequently their effectiveness against impact and wear [7]. Another important aspect is their thickness because the greater the thickness, the greater the protection (chemical, mechanical, and thermal) they will provide. When deposited by dip-coating, the thickness of the resulting coating depends on the physicochemical properties of the sol-gel solution (density, viscosity, pH, etc.) and on the deposition conditions (especially on the rate of withdrawing the substrate from the sol-gel solution).

Unfortunately, unlike other coating techniques as for example chemical vapour deposition, physical vapour deposition, electrophoretic deposition, and plasma-spray [8], which routinely get coatings with thicknesses from a few to tens of microns, it is not easy to obtain thick sol-gel coatings of quality because there is a certain critical thickness (t_c) above which the coating cracks. In particular, t_c is defined as the greatest possible thickness of the crack-free monolayer coating [9]. In order to obtain coatings that are thicker, multilayer coatings must be prepared by successively depositing as many individual layers as needed within what is possible. This will ensure that each individual

* Corresponding author.
E-mail address: alortiz@unex.es (A.L. Ortiz).

https://doi.org/10.1016/j.ceramint.2020.04.028
Received 26 November 2019; Received in revised form 3 March 2020; Accepted 3 April 2020
0272-8842/ © 2020 Elsevier Ltd and Techna Group S.r.l. All rights reserved.

layer is crack-free [10], and that the multilayer coating has the desired total thickness.

There have been many studies on obtaining and characterizing sol-gel ceramic coatings on metallic substrates [11,12], but fewer on ceramic substrates. Moreover, most earlier studies have investigated, to a greater or lesser extent, the effect of both intrinsic (viscosity, oxide concentration, pH, etc.) and extrinsic (withdrawal rate, atmosphere, etc.) factors involved in the sol-gel method on the features and properties of resulting coatings [13,14]. However, little is known on how the substrate itself conditions the layers that can be deposited on it. Motivated by this paucity, in the present work therefore, 3YSZ multilayer sol-gel coatings were deposited on different substrates in order to study the influence of the substrate and the sintering temperature on (*i*) the thickness and quality of the monolayer coatings, and (*ii*) the maximum number of layers that can be deposited without the coating cracking. In particular, the substrates chosen were stainless steel AISI-310, soda-lime glass, fused quartz, and sapphire. They were not selected arbitrarily, but based on scientific and practical motivations. The former is to have a set of four substrates whose thermal expansion coefficients are much lower (fused quartz), lower but comparable (sapphire and soda-lime glass), and muck higher (AISI-310) than that of 3YSZ coating. The latter is to conduct the study on substrates of different natures (metallic and ceramics) and states (amorphous and crystalline), which are also being coated due to different interests (to provide thermal, anti-wear/impact, and anti-corrosion/oxidation protections, to impart specific optical properties, etc.). Thus, the study seeks to establish guidelines for the design of better thick sol-gel ceramic coatings deposited on very diverse substrates because the thickness of the monolayers and the maximum number of monolayers possible are key factors for the sol-gel coatings to offer the desired functionality and durability.

2. Experimental methods

2.1. Preparation of the 3YSZ solution

Two precursor solutions, one of ZrO_2 and the other of Y_2O_3, were prepared and mixed in adequate proportions to yield a 3YSZ solution. The ZrO_2 solution was prepared by dissolving zirconium(IV) n-propoxide (ZNP; 70 wt% diluted) in propanol (PrOH) and nitric acid (HNO_3) in an anhydrous N_2 atmosphere (to avoid hydroxide precipitation). The Y_2O_3 solution was prepared by dissolving yttrium(III) acetate ($YAc{\cdot}4H_2O$) in PrOH and HNO_3. The ZNP/PrOH/H_2O/HNO_3 molar ratios of the 3YSZ solution were 1/15/6/1 [9]. This solution is stable, clear, and transparent, and at room temperature has a density of 0.885 g/cm^3, viscosity of 5.1 cP, and pH of 0.5 in fresh conditions.

2.2. Deposition and characterization of the coatings

Four commercially available (Goodfellow Ltd.) substrates were used – three transparent (soda-lime glass, fused quartz, and sapphire) and one opaque (stainless steel AISI-310). They were all cleaned before use, and the AISI-310 substrate was also polished to 1-μm finish (the transparent substrates were received already polished).

Firstly, the 3YSZ solution was deposited on the substrates in air at room temperature by dip-coating using different withdrawal rates (10–20 cm/min) to thus identify which was optimal. The 3YSZ solution was then deposited on the substrates at this optimal withdrawal rate, at ambient conditions, and the fresh coatings were dried in air at 100 °C for 1 h. This is to remove both water and solvents used for preparing the sol-gel solutions. Next, they were sintered in air at 300 °C, 500 °C, or 800 °C (except for the soda-lime glass) for 2 h, using heating and cooling rates of 3 °C/min. These temperatures were selected (*i*) to obtain coatings of different natures (amorphous at 300 °C, partially crystalline at 500 °C, and crystalline at 800 °C) and degrees of porosity [13], and (*ii*) to cover the temperature range of application of the typical metallic substrates. This entire process was repeated as many times as possible until the multilayer coating cracked spontaneously.

The 3YSZ coatings deposited on transparent substrates were characterized by transmittance spectroscopy (Helios Alpha UV–Vis spectrophotometer, Thermo Fisher Scientific). Specifically, transmittance spectra were recorded for coatings on soda-lime glass, fused quartz, and sapphire substrates over the spectral range 200–1000 nm, from which the refractive indices of the coatings were calculated and used to compute their thickness and porosity by the Swanepoel method [15,16]. The thickness of the coatings on the non-transparent AISI-310 substrate was measured by mechanical profilometry (Hommel Tester T2 Profilometer), and their porosity from the thicknesses as described elsewhere [17]. All 3YSZ coatings were characterized by optical microscopy (Epiphot 300, Nikon). These observations were made to check for the possible spontaneous cracking of the coatings each time that a new layer was deposited and sintered. Finally, selected coatings were also characterized by X-ray diffractometry (XRD; PW-1800, Philips Research laboratory). The XRD patterns were collected using Cu-Kα incident radiation over the angular range 26–62° 2θ, and were compared to analyse how the peak shifting was affected by the substrate and sintering temperature.

3. Results and discussion

Obtaining quality coatings by dip-coating requires first determining the critical withdrawal rate (v_c) which is applicable during the deposition stage that will lead to films that are both crack-free and as thick as possible. It is known that v_c depends on the physicochemical properties of the sol-gel solutions used, especially on their viscosity (η) [9]. In practice, due to the aging of the solutions over time, it is found best to determine the product $v_c{\cdot}\eta$ because this remains constant as long as the aging time of the sol-gel solution is not excessive. In the present case, it was determined experimentally that, at room temperature, $v_c{\cdot}\eta$ is 85 cm cP/min. This was done by first measuring the viscosity of the fresh solution by an Ostwald viscometer (5.1 cP), and then by dip-coating this solution under increasingly withdrawal rates up to the first observation of cracks (~16.7 cm/min) in the coatings dried at 100 °C.

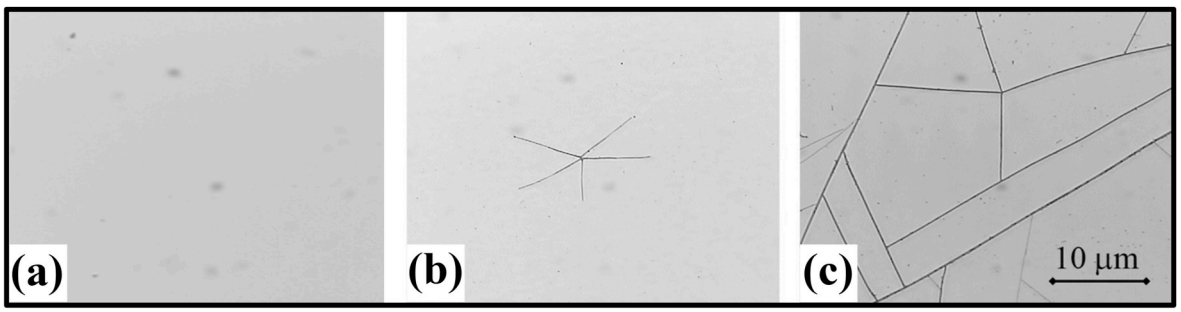

Fig. 1. Optical micrographs of monolayer 3YSZ coatings deposited on soda-lime glass at withdrawal rates (a) slower (15 cm/min), (b) slightly faster (17 cm/min) and (c) much faster (19 cm/min) than critical (~16.7 cm/min). The scale bar is the same for the three micrographs.

Fig. 1 shows optical micrographs of 3YSZ monolayer coatings on soda-lime glass substrates prepared both at one withdrawal rate lower (i.e., 15 cm/min) than v_c (~16.7 cm/min) and at two withdrawal rates (i.e., 17 and 19 cm/min) greater than v_c, and then dried at 100 °C. One sees that the coating deposited at withdrawal rate below v_c is free of cracks (Fig. 1a). One also sees that, while the two coatings deposited with the withdrawal rates above v_c are cracked, the cracking is only light for the withdrawal rate just above v_c (~0.3 cm/min above; Fig. 1b), but total for the withdrawal rate that is much faster than v_c (~2.2 cm/min above; Fig. 1c). Since this cracking is irreversible (the cracks, however small, do not disappear when new layers are deposited on top), it is especially important to never exceed v_c to prepare sol-gel coatings of quality.

First the 3YSZ solution was prepared and characterized, and the aging-dependent behaviour of v_c was determined. Then monolayer and bilayer coatings were deposited on substrates of fused quartz, sapphire, soda-lime glass, and AISI-310. A withdrawal rate of 16 cm/min, which is slightly lower than v_c, was used so as to obtain crack-free layers as thick as possible. These were analysed by the Swanepoel method (transparent substrates) [15,16] or by mechanical profilometry (the non-transparent substrate). By way of example, Fig. 2 shows curves of transmittance *vs* wavelength ($T(\lambda)$) of some coatings prepared under the same deposit (16 cm/min) and heat treatment conditions (500 °C) for the three transparent substrates, showing the expected interference bands. In Swanepoel's method, the refractive index of the coating (n) is calculated from the transmittance data in the region of weak absorption of the spectrum (λ = 500–800 nm) by the expression [16]:

$$n(\lambda) = \sqrt{N + \sqrt{N^2 - s^2}}$$

where s is the refractive index of the substrate, and N is given by:

$$N = 2s\frac{T_M - T_m}{T_M\ T_m} + \frac{s^2 + 1}{2}$$

where T_M and T_m are the envelopes of the maxima and minima, respectively, of the interference bands. From n, one then determines the thickness (t) and porosity (P) of each monolayer/multilayer coating by means of the expressions [16]:

$$t = \frac{M\lambda_1\lambda_2}{2[\lambda_1 n(\lambda_2) - \lambda_2 n(\lambda_1)]}$$

$$P = 1 - \frac{n^2(\lambda) - 1}{n_d^2(\lambda) - 1}$$

where M = 1 for two adjacent extremes of the same type (maximum-maximum or minimum-minimum) and M = 1/2 for two adjacent extremes of different types (maximum-minimum or minimum-maximum), as well as $n(\lambda)$ and $n_d(\lambda)$ being the refractive indices of the porous and dense coatings, respectively. Swanepoel's method is not however applicable to coatings on opaque substrates. Therefore, the thicknesses (t) of the coatings on AISI-310 were measured directly by mechanical profilometry, and their porosities were estimated using the expression [17]:

$$P = 1 - \frac{t_d}{t}$$

where t_d is the thickness of the dense coating. By way of example, Table 1 gives the P and t values of the monolayer and bilayer coatings deposited on the four substrates (16 cm/min withdrawal rate, and dried at 100 °C) and then sintered at 500 °C, as well as each substrate's thermal expansion coefficient. One observes that the coatings are porous, with similar but not quite equal degrees of porosity (between 27% and 23.5%). This is because P depends primarily on the sintering temperature [18,19], but only secondarily on the substrate (with the substrate's thermal expansion coefficient, the lower the porosity of the coatings). One also observes that, within the errors, bilayer coatings are twice as thick as monolayer coatings, indicating that the thickness of each individual layer of a multilayer coating will always be practically the same for a given substrate. From the table, one observes that the substrate affected the coatings' thickness despite the deposit, drying, and sintering conditions being identical. In particular, the greater the substrate's thermal expansion coefficient, the greater the thickness of the coatings, with the difference reaching 13% in the thickness of the monolayer between the extreme cases (fused quartz and AISI-310 substrates).

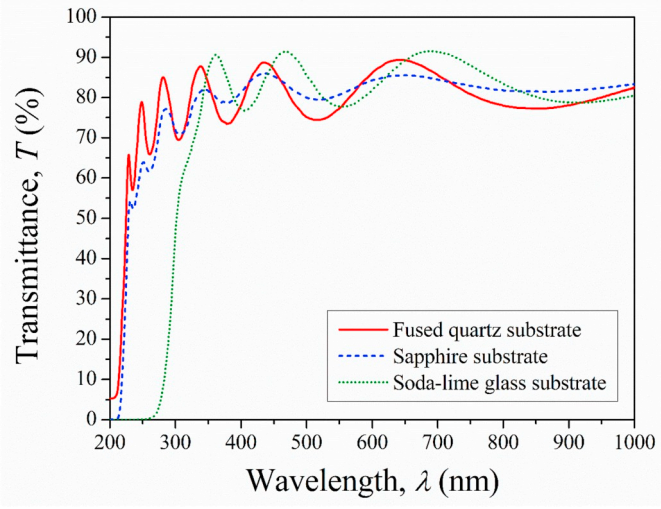

Fig. 2. Transmittance *vs* wavelength spectra of bilayer 3YSZ coatings deposited on fused quartz, sapphire, and soda-lime glass transparent substrates at a withdrawal rate of 16 cm/min, dried at 100 °C, and sintered at 500 °C.

Table 1
Porosity (P) and thickness (t) of the monolayer and bilayer coatings deposited at a withdrawal rate of 16 cm/min, dried at 100 °C, and sintered at 500 °C, and the thermal expansion coefficient of the different substrates used.

Substrate	Porosity, P (%)[a]	Coating thickness, t (nm)[a]		Thermal expansion coefficient, (°C^{-1})
		Monolayer	Bilayer	
Fused quartz	27	175	348	0.8×10^{-6}
Sapphire	24	183	366	8.8×10^{-6}
Soda-lime glass	24	185	370	9.0×10^{-6}
AISI-310	23.5	198	396	16.0×10^{-6}

[a] The errors of P and t are ± 2%.

The same is the case with the number of layers that can be deposited on each substrate for a given sintering temperature. Table 2 lists the maximum number of layers of crack-free multilayer coatings that were sintered at 300 °C, 500 °C, and 800 °C. As before, one also observes in the table that, for a given sintering temperature, the number of layers deposited increased as the substrate's thermal expansion coefficient increased. This effect becomes much more pronounced with increasing sintering temperature. Furthermore, other two observations with increasing sintering temperature are that the number of layers deposited on any given substrate also increased, and that the differences in this number between substrates became more pronounced as well.

The explanation of these experimental observations (thickness of each individual layer, and maximum number of layers possible) lies in the residual in-plane stresses (σ_R) generated during cooling from the sintering temperature down to room temperature (ΔT). These in-plane stresses are a result of the difference between the thermal expansion coefficients of the substrate and coating ($\Delta\alpha$) during cooling. In particular, σ_R depends on the substrate and the sintering temperature as: $\sigma_R \propto \Delta\alpha \cdot \Delta T$. In principle, it is to be expected that the greater the residual in-plane compressive stress on the coating, the more layers it would be possible to deposit, and hence the thicker the resulting multilayer coating. The opposite trend would be the case if the residual in-plane

ARTICLE IN PRESS

Table 2
Number of crack-free layers that could be deposited on the different substrates (withdrawal rate of 16 cm/min, and drying at 100 °C), product $\Delta\alpha\cdot\Delta T$, and residual porosity for the different sintering temperatures.

Substrate	Number of crack-free layers			$\Delta\alpha\cdot\Delta T$[a]			Porosity, P (%)[b]		
	300 °C	500 °C	800 °C	300 °C	500 °C	800 °C	300 °C	500 °C	800 °C
Fused quartz	2	2	3	$+2.53\times10^{-3}$	$+4.37\times10^{-3}$	$+7.13\times10^{-3}$	30	27	24
Sapphire	3	6	12	$+3.30\times10^{-4}$	$+5.70\times10^{-4}$	$+9.30\times10^{-4}$	28	24	21
Soda-lime glass	3	7	–	$+2.75\times10^{-4}$	$+4.75\times10^{-4}$	$+7.75\times10^{-4}$	27	24	19.5
AISI-310	3	10	≥18	-1.65×10^{-3}	-2.85×10^{-3}	-4.65×10^{-3}	27	23.5	19

[a] The signs + and - indicate residual in-plane tensile and compressive stresses, respectively.
[b] The error of P is ± 2%. Note that the substrate of soda-lime glass cannot be heat treated at 800 °C.

stresses on the coating are tensile. Indeed, the multilayer coatings cracked at smaller number of layers (hence smaller total thickness) when the substrate's thermal expansion coefficient was much lower than that of 3YSZ ($\sim10\times10^{-6}$ °C^{-1}), as for example in the case of fused quartz ($\sim0.8\times10^{-6}$ °C^{-1}), because in this scenario the coatings are subject to greater residual in-plane tensile stresses (Table 2) that facilitate the appearance and propagation of cracks. Logically, as the substrate's thermal expansion coefficient approaches that of 3YSZ, more layers could be deposited because the residual in-plane tensile stresses on the coating decreased, as inferred from Table 2 in comparing the cases of fused quartz ($\sim0.8\times10^{-6}$ °C^{-1}), sapphire ($\sim8.8\times10^{-6}$ °C^{-1}), and soda-lime glass ($\sim9.0\times10^{-6}$ °C^{-1}). Finally, one sees that the most favourable scenario is when the substrate has a thermal expansion coefficient greater than that of 3YSZ, as is the case of AISI-310 ($\sim16\times10^{-6}$ °C^{-1}), because then the coating is subjected to residual in-plane compressive stresses (Table 2) that hinder the appearance and propagation of cracks.

The effect of increasing the sintering temperature is striking because in all cases the number of layers also increased. This was to be expected for the AISI-310 substrate because the residual in-plane compressive stresses on the coating increase (Table 2). But the trend was surprising for the fused quartz, sapphire, and soda-lime glass substrates because in these cases it is their residual in-plane tensile stresses which increase (Table 2), and this should have facilitated cracking in the coatings. The explanation is that the coatings are not fully dense, and the increase in their densification dominates the in-plane tensile stresses. In particular, the decrease in residual porosity of the coatings (Table 2) reduces the population of nuclei for the appearance and propagation of cracks, making the coating more resistant to cracking despite being subjected to a greater residual in-plane tensile stress.

The above arguments were validated qualitatively by XRD. By way of example, Fig. 3 compares the XRD patterns of three selected coatings. One observes that the 3YSZ XRD peaks are shifted towards smaller diffraction angles for the coating on the substrate with the greater thermal expansion coefficient (i.e., AISI-310), with the higher sintering temperature (i.e., 800 °C) causing greater shift. Thus for example, 111 peak of 3YSZ is located ~30.77°2θ in the coating deposited on the soda-lime glass substrate at 500 °C, but at ~30.65°2θ and ~30.52°2θ in the coatings deposited on the AISI-310 substrate at 500 °C and 800 °C, respectively. The same trends are applicable to the 220 and 311 peaks, but with different the absolute shifts depending on the Miller indices. What is relevant is that these shifts in the XRD patterns constitute experimental evidence for greater residual in-plane compressive stresses or lower residual in-plane tensile stresses in the coating. Indeed, residual in-plane compressive stresses in the coating cause the 3YSZ crystalline structure to contract in-plane, thus causing out-of-plane elongation (correlated by the material's Poisson ratio), with the greater in-plane compressive stress corresponding to greater out-of-plane elongation. In accordance with Bragg's law ($2d_{hkl}\sin\theta = \lambda$), the greater value of the 3YSZ out-of-plane interplanar spacings (d_{hkl}) means that its XRD peaks shift towards smaller diffraction angles. The opposite is the case if the residual in-plane stresses in the coating are tensile because

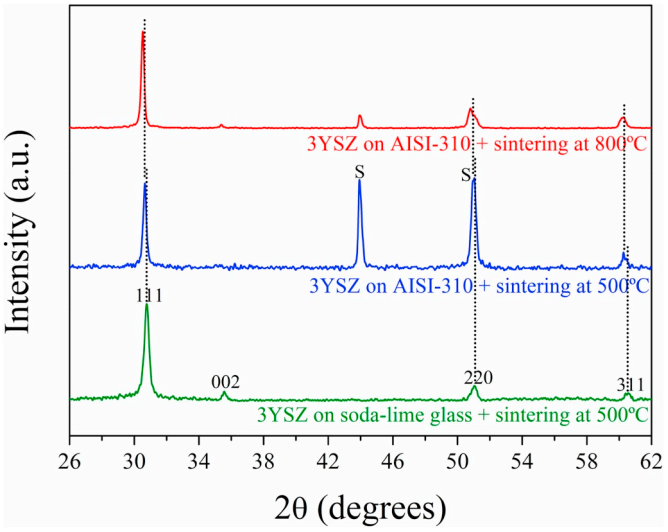

Fig. 3. XRD patterns of 3YSZ coatings deposited on soda-lime glass and then sintered at 500 °C, and on AISI-310 and then sintered at 500 °C and 800 °C. The 3YSZ (cubic polymorph) Miller indices are indicated. *S* denotes the substrate's XRD peaks. The vertical dotted lines are to guide the eye in observing the shifts of the peaks.

then the 3YSZ crystalline structure is stretched in-plane and contracted out-of-plane. The XRD results thus confirm the residual in-plane stresses explanation of the trends in the thickness of the layers and the number of layers that can be deposited on each substrate.

4. Conclusions

3YSZ multilayer sol-gel coatings were deposited on four different substrates. They were sintered at different temperatures, and the thickness of each individual layer and the number of layers that could be deposited without the multilayer coating cracking were determined. The following conclusions can be drawn from the experimental observations and the analyses:

1. All the layers of a multilayer sol-gel coating have the same thickness (if the sintering temperature is constant). However, a substrate with a greater thermal expansion coefficient permits the layers to be thicker.
2. The maximum possible number of layers of the multilayer sol-gel coating increases with greater values of the substrate's thermal expansion coefficient and with higher sintering temperatures. The former is because there is a reduction/increase in the residual in-plane tensile/compressive stresses in the coating. The latter is because the densification of the layers either predominates over the increased in-plane tensile stresses or combines synergistically with the greater in-plane compressive stresses.

Declaration of competing interest

The authors declare that they have no known competing financial interests or personal relationships that could have appeared to influence the work reported in this paper.

Acknowledgements

This work was supported by the Junta de Extremadura and FEDER Funds under the grant number GR18164.

References

[1] M. Atik, M.A. Aegerter, Corrosion-resistant sol-gel ZrO_2 coatings on stainless-steel, J. Non-Cryst. Solids 147 (1992) 813–819.
[2] P.D. Neto, M. Atik, L.A. Avaca, M.A. Aegerter, Sol-gel coatings for chemical protection of stainless steel, J. Sol. Gel Sci. Technol. 2 (1994) 529–534.
[3] V. Encinas-Sánchez, A. Macías-García, M.A. Díaz-Díez, A. Díaz-Parralejo, Characterization of sol–gel coatings deposited on a mechanically treated stainless steel by using a simple non-destructive electrical method, J. Ceram. Soc. Jpn. 124 (2016) 185–191.
[4] H. Dislich, L.C. Klein (Ed.), Sol-Gel Technology for Thin Films, Fibers, Performs, Electronics and Specialty Shapes, N.J. Noyes, 1988.
[5] C.Y. Fong, S.S. Ng, F.K. Yam, H. Abu Hassan, Z. Hassan, Growth of GaN on sputtered GaN buffer layer via low cost and simplified sol-gel spin coating method, Vacuum 119 (2015) 119–122.
[6] E.R. Rwenyagila, B. Agyei-Tuffour, M.G. Zebaze Kana, O. Akin-Ojo, W.O. Soboyejo, Optical properties of ZnO/Al/ZnO multilayer films for large area transparent electrodes, J. Mater. Res. 29 (24) (2015) 2912–2920.
[7] F. Blas, F. Ansart, P. Lours, J.P. Bonino, S. Duluard, V. Vidal, L. Pin, G. Pujol, L. Bonin, Processing thermal barrier coatings via sol-gel route: crack network control and durability, Surf. Coating. Technol. 334 (2018) 71–77.
[8] B.H. Jeong, S.M. Park, W.S. Hwang, K.H. Hyun, Y.O. Park, T.K. Jung, S.K. Hyun, Thermal properties of plasma-sprayed multilayer Al_2O_3/yttria-stabilized zirconia coating, J. Nanosci. Nanotechnol. 20 (2020) 524–529.
[9] A. Díaz-Parralejo, A. Macías-García, J. Sánchez-González, M.A. Díaz-Díez, E.M. Cuerda-Correa, Influence of the experimental parameters on the synthesis process of yttria-doped zirconia sol-gel films, Surf. Coating. Technol. 204 (14) (2010) 2257–2261.
[10] A.K. Stamper, D.W. Greve, T.E. Schlesinger, Deposition of textured yttria-stabilized ZrO_2 films on oxidized silicon, J. Appl. Phys. 70 (1991) 2046–2051.
[11] A. Díaz-Parralejo, A. Macías-García, M.A. Díaz-Díez, V. Encinas Sánchez, J.P. Carrasco-Amador, Preparation and characterization of multilayer coatings on tool steel, Ceram. Int. 45 (14) (2019) 16934–16939.
[12] S. Senani, E. Campazzi, M. Villatte, C. Druez, Potentiality of UV-cured hybrid sol-gel coatings for aeronautical metallic substrate protection, Surf. Coating. Technol. 227 (2013) 32–37.
[13] R. Caruso, A. Díaz-Parralejo, P. Miranda, F. Guiberteau, Controlled preparation and characterization of multilayer sol-gel zirconia dip-coatings, J. Mater. Res. 16 (2001) 2391–2398.
[14] A. Díaz-Parralejo, A.L. Ortiz, R. Caruso, Effect of sintering temperature on the microstructure and mechanical properties of ZrO_2-3 mol%Y_2O_3 sol-gel films, Ceram. Int. 36 (2010) 2281–2286.
[15] R. Swanepoel, Determination of the thickness and optical-constants of amorphous-silicon, J. Phys. E Sci. Instrum. 16 (12) (1983) 1214–1222.
[16] J. Sánchez-González, A. Díaz-Parralejo, A.L. Ortiz, F. Guiberteau, Determination of optical properties in nanostructured thin films using the Swanepoel method, Appl. Surf. Sci. 252 (2006) 6013–6017.
[17] A. Díaz-Parralejo, R. Caruso, A.L. Ortiz, F. Guiberteau, Densification and Porosity evaluation of ZrO_2-3mol% Y_2O_3 sol-gel thin films, Thin Solid Films 458 (2004) 92–97.
[18] A. Ayral, A. El Mansouri, M.P. Vieira, C. Pilon, Porosity of sol-gel derived silica coatings on glass substrates, J. Mater. Sci. Lett. 17 (1998) 883–885.
[19] Y. Tamar, M. Kahanov, C. Haspel, Y. Sasson, Size selectivity during dip coating of sol-gel silica-based antireflective coatings and its effect on the porosity of the coatings, J. Coating Technol. Res. 13 (6) (2016) 1103–1113.